Journal of Mathematical Modeling
Vol. -, No. -, 2022, pp. -, Research article.

JMM

A finite element approximation of a current-induced magnetization dynamics model

Mohammed Moumni*, Mouhcine Tilioua

MAIS Laboratory, MAMCS Group, FST Errachidia, Moulay Ismail University of Meknes, P.O. Box: 509 Boutalamine, 52000 Errachidia, Morocco
Email(s): md.moumni@gmail.com, m.tilioua@fste.umi.ac.ma

Abstract. Micromagnetics is a continuum theory describing magnetization patterns inside ferromagnetic media. The dynamics of a ferromagnetic material are governed by the Landau-Lifshitz equation. This equation is highly nonlinear and has a non-convex constraint. In this work, a finite element approximation of a current-induced magnetization dynamics model is proposed. The model consists of a modified Landau-Lifshitz-Gilbert (LLG) equation incorporating spin transfer torque. The scheme preserves a non-convex constraint, requires only a linear solver at each time step and is easily applicable to the limiting cases. As the time and space steps tend to zero, a proof of convergence of the numerical solution to a (weak) solution of the modified LLG equation is given. Numerical results are presented to show the effect of the injected current on magnetization switching.

Keywords: Ferromagnetism, magnetization dynamics, spin polarized current, finite elements.
AMS Subject Classification : 78A25, 35Q60, 35B40, 35K55, 65M12, 65M60.

1 Introduction

It has been recently shown, both theoretically and experimentally, that a spin polarized current when passing through a small magnetic conductor can affect its magnetization state. The interaction between spin polarized current and magnetization in small ferromagnetic bodies can produce steady state precessional magnetization dynamics, that is self-oscillating behavior, or even the switching of magnetization direction [7, 35]. Both types of dynamical behavior have potential applications in magnetic storage technology and spintronics. In this respect, it was predicted, and later confirmed, that spin-polarized current can lead to current-controlled hysteretic switching in magnetic nanostructures. This kind of behavior may become very important for applications such as current-controlled switching of magnetic random

*Corresponding author.
Received: 29 April 2021/ Revised: 31 May 2021/ Accepted: 2 June 2021
DOI: 10.22124/jmm.2021.19486.1673

access memory elements and stabilization of magnetic hard-disk read heads. Steady precessional oscillations of magnetization due to spin polarized currents have also interesting potential applications for the realization of current-controlled microwave oscillators integrable with semiconductor electronics. This kind of oscillators could be used to realize a very new design of clocks for synchronization of electronic devices. In this work, we investigate magnetization switching under the influence of a spin-polarized current through numerical simulations using a generalized LLG equation incorporating spin transfer torque effect. To describe the model equations we consider Ω a bounded and regular open set of $\mathbb{R}^3$. The generic point of $\mathbb{R}^3$ is denoted by x. We assume that a ferromagnetic material occupies the domain Ω. With a prescribed current density $J(t,x)$, the time evolution of the magnetization vector $\boldsymbol{m}(t,x)$ may be described by the LLG equation, see for example [20, 35]

$$\partial_t \boldsymbol{m} - \alpha \boldsymbol{m} \times \partial_t \boldsymbol{m} = -\gamma \boldsymbol{m} \times (\mathscr{H}_e + \beta (J \cdot \nabla) \boldsymbol{m}), \tag{1}$$

in $Q = (0,T) \times \Omega$ where $T > 0$ is fixed and "$\times$" denotes the cross product in $\mathbb{R}^3$. The term parameterized by the positive factor α describes (Gilbert) damping torque. The first term on the right-hand side accounts for torque by the effective field $\mathscr{H}_e$ which is given by

$$\mathscr{H}_e(\boldsymbol{m}) = \triangle \boldsymbol{m} + \nabla \varphi,$$

where φ satisfies the stray field equation

$$\operatorname{div}(\nabla \varphi + \boldsymbol{m}) = 0 \text{ in } (0,T) \times \mathbb{R}^3.$$

The term parameterized by the positive constant β expresses current-induced torques on $\boldsymbol{m}$. This torque is most commonly termed non-adiabatic and β characterizes its strength. The parameter $\gamma > 0$ is a gyroscopic ratio. The initial data satisfied by the magnetization is

$$\boldsymbol{m}(0,x) = \boldsymbol{m}_0(x), \;\; |\boldsymbol{m}_0(x)|^2 = 1 \text{ a.e. in } \Omega.$$

Equation (1) should be solved together with appropriate boundary conditions for the magnetization. We consider homogeneous Neumann boundary condition

$$\partial_n \boldsymbol{m} = 0 \text{ on } (0,T) \times \partial\Omega. \tag{2}$$

Equation (1) without injected current ($\beta = 0$) have already been substantially studied in the literature and solutions have been found:

- either in a strong sense [8] but only locally in time, or globally but for initial data of small energy and in 2D;
- either in a weak sense [3] and [38]. In that case, solutions are shown to be global in time but may not be unique (explicit cases of nonuniqueness are provided in [3]).

Global existence of weak solutions for the problem (1) was addressed by Tilioua [37]. Recently, a generalization of (1) to adiabatic spin torque is considered by Melcher-Ptashnyk [27]. This torque takes the form $\boldsymbol{m} \times J \cdot \nabla \boldsymbol{m}$ and is added to effective field.

Since we will focus on only the effects of the injected current and for the sake of simplicity we shall neglect here the demagnetizing field $\nabla\varphi$ and we refer for example to [22] for some computational aspects of this field. However, we note that this simplification does not limit the proposed analysis.

The study of the solutions of the nonlinear PDEs are significant and a vital topic in real life, due to its enormous contribution to science and technology. In the past, the development of mathematical algorithms to seek these solutions very difficult, but with the development of science it became possible. An operational matrix-based spectral computational method coupled with the Picard technique and successfully employed to seek the solutions to a family of nonlinear evolution differential equations and the nonlinear oscillatory fractional order differential equations [10–13]. The soliton based algorithms are also promising techniques to analyze the solutions of various nonlinear real-world problems [14]. The Monte Carlo algorithm, finite-difference scheme, finite element method, mixed finite element method and the neural network approximation give a good results to solve nonlinear PDEs, stochastic PDEs and the PDEs in the high dimension, see [17–19, 25, 26, 28–33, 39]. In this study we use the finite element method to solve our problem because it has a lot of avantages for examples:

- **Modeling.** FEM allows for easier modeling of complex geometrical and irregular shapes. Because the designer is able to model both the interior and exterior, he or she can determine how critical factors might affect the entire structure and why failures might occur.

- **Adaptability.** FEM can be adapted to meet certain specifications for accuracy in order to decrease the need for physical prototypes in the design process. Creating multiple iterations of initial prototypes is usually a costly and timely process. Instead of spending weeks on hard prototyping, the designer can model different designs and materials in hours via software.

- **Accuracy.** While modeling a complex physical problem by hand can be impractical, a computer using FEM can solve the problem with a high degree of accuracy.

- **Time-dependent simulation.** FEM is highly useful for certain time-dependent simulations, such as crash simulations, in which deformations in one area depend on deformation in another area.

- **Boundaries.** With FEM, designers can use boundary conditions to define to which conditions the model needs to respond. Boundary conditions can include point forces, distributed forces, thermal effects (such as temperature changes or applied heat energy), and positional constraints.

- **Visualization.** Engineers can easily spot any vulnerability in design with the detailed visualizations FEM produces, then use the new data to make a new design.

Before dealing with the finite elements discretization of the problem (1)-(2), let us first review some previous results. We limit ourselves to mention a handful of references concerning numerical aspects and we refer to the survey [21] for a more detailed bibliographical account. The general framework (although without injected current, i.e. the case $\beta = 0$) has been established in earlier papers. For instance Banas et al. [4] has proposed an implicit nonlinear scheme to solve problem (1), and prove that the finite element solution converges to a weak global solution of the problem. Their method requires a condition on the time step k and space step h (namely $k = o(h^2)$) for the convergence of the nonlinear system of equations resulting from the discretization. This method gives an approximated sequence of solutions converging to a global solution of the problem. Next, following the idea developed by Alouges and Jaisson [2] (see

also Alouges [1]) for the LLG equation (1), Le and Tran [23] proposed a θ-linear finite element scheme to find a weak global solution to (1) always with $\beta = 0$, but coupled to magnetostatic approximation of the magnetic field. It is proved that the numerical solutions converge to a weak solution of the problem with no condition imposed on time step and space step as $\theta \in (1/2, 1]$. It is required that $k = o(h^2)$ when $\theta \in [0, 1/2)$, and $k = o(h)$ when $\theta = 1/2$. In this work, we shall adapt the scheme proposed in [4] to deal with non-adiabatic spin transfer torque model (1).

The paper is organized as follows. Weak solutions of the modified LLG equations are defined in Section 2 in which we also recall a global existence result. Following Alouges [1], Le [23] and Tran [24], we introduce in section 3 the θ-linear finite element scheme. Section 4 is devoted to convergence of the finite element solutions to a weak solution of the LLG equations. The main ingredient of the convergence proof is the Lemma 3 which provides L^2-bounds for the discrete solutions. In order to show the effect of the injected current on magnetization dynamics, a set of numerical experiments is provided in Section 5. We conclude the paper in the last section by giving some comments and directions for future development.

Throughout, we make use of the following notations. $Ł^2(\Omega) = (L^2(\Omega))^3$ and $\mathbb{H}^1(\Omega) = (H^1(\Omega))^3$ are the vector-valued Hilbert spaces equipped with the norm $|\cdot|_\Omega$ and $\|\cdot\|$, respectively. $(L^\infty(\Omega))^3$ is denoted by $Ł^\infty(\Omega)$ with norm $|\cdot|_\infty$. We denote $\langle\cdot,\cdot\rangle_\omega := \langle\cdot,\cdot\rangle_{\mathbb{L}^2(\omega)}$.

2 Weak formulation and global existence result

We first state the definition of weak solutions to problem (1).

Definition 1. *Given $\boldsymbol{m}_0 \in \mathbb{H}^1(\Omega)$ such that $|\boldsymbol{m}_0| = 1$ a.e in Ω, we call $\boldsymbol{m}(t,x)$ a weak solution to the LLG equation (1) if for all $T > 0$, there hold*

1. *For all $T > 0$, $\boldsymbol{m} \in \mathbb{H}^1(Q)$ and $\boldsymbol{m}$ satisfies the saturation constraint $|\boldsymbol{m}(t,x)| = 1$ for a.e in Q.*
2. *$\boldsymbol{m}(0,\cdot) = \boldsymbol{m}_0(\cdot)$ in the trace sense.*
3. *For all $\boldsymbol{G} \in (\mathscr{C}^\infty(Q))^3$, there holds*

$$\langle \partial_t \boldsymbol{m}, \boldsymbol{G}\rangle_Q - \alpha \langle \boldsymbol{m} \times \partial_t \boldsymbol{m}, \boldsymbol{G}\rangle_Q = -\gamma \langle \nabla \boldsymbol{m}, \nabla(\boldsymbol{m} \times \boldsymbol{G})\rangle_Q - \gamma\beta \langle \boldsymbol{m} \times (J \cdot \nabla \boldsymbol{m}), \boldsymbol{G}\rangle_Q .$$

4. *For all $t \geq 0$, we have*

$$\mathscr{E}(t) + \frac{\alpha}{\gamma} \int_0^t \int_\Omega |\partial_t M|^2 \, \mathrm{d}x\mathrm{d}t \leq \mathscr{E}(0)(1 + I(t)\exp(I(t))),$$

where

$$\mathscr{E}(t) = |\nabla \boldsymbol{m}(t)|_\Omega^2,$$

and

$$I(t) = \frac{\gamma\beta^2}{\alpha} \int_0^t |J|_\infty^2 \mathrm{d}s,$$

for all $t \in (0, T)$.

We have the following global existence result (see Tilioua [37]).

Theorem 1. *Let $T>0$ be fixed and $\boldsymbol{m}_0 \in \mathbb{H}^1(\Omega)$ be such that $|\boldsymbol{m}_0(x)|^2 = 1$ a.e. Assume that J belongs to $L^2(0,T;\mathbb{L}^\infty(\Omega))$. Then there exists a global weak solution $\boldsymbol{m}$ of the problem (1)-(2) in the sense of Definition 1.*

3 The finite elements discretization

In the spirit of [1], see also [5, 23], we introduce a θ-linear finite element scheme which approximates a weak solution $\boldsymbol{m}$ defined in Definition 1. Let $\mathscr{T}_h$ be a regular triangulation of the domain Ω parameterized by mesh-size h. We denote by $\mathscr{N}_h := \{\boldsymbol{x}_1,\ldots,\boldsymbol{x}_N\}$ the set of vertices, they are not distinct and by $\mathscr{M}_h := \{e_1,\ldots,e_M\}$ the set of edges.

To discretize the LLG equation (1), we introduce the finite element space $\mathbb{V}_h \subset \mathbb{H}^1(\Omega)$ which is the space of all continuous piecewise linear functions on $\mathscr{T}_h$. A basis for $\mathbb{V}_h$ can be chosen to be $(\phi_n)_{1\le n\le N}$, where $\phi_n(\boldsymbol{x}_m) = \delta_{n,m}$. Here $\delta_{n,m}$ stands for the Kronecker symbol. The interpolation operator from $\mathscr{C}^0(\Omega,\mathbb{R}^3)$ onto $\mathbb{V}_h$ is denoted by $I_{\mathbb{V}_h}$,

$$I_{\mathbb{V}_h}(\boldsymbol{v}) = \sum_{n=1}^{N} \boldsymbol{v}(x_n)\phi_n(x) \quad \forall \boldsymbol{v} \in \mathscr{C}^0(\Omega,\mathbb{R}^3).$$

Fixing a positive integer M, we choose the time step k to be $k = T/M$ and define $t_j = jk$, $j = 0,\ldots,M$. For $j = 1,2,\ldots,M$, the functions $\boldsymbol{m}(t_j,\cdot)$ is approximated by $\boldsymbol{m}_h^{(j)} \in \mathbb{V}_h$.

We define the space $\mathbb{W}_h^{(j)}$ by

$$\mathbb{W}_h^{(j)} := \left\{ \boldsymbol{w} \in \mathbb{V}_h \mid \boldsymbol{w}(\boldsymbol{x}_n)\cdot \boldsymbol{m}_h^{(j)}(\boldsymbol{x}_n) = 0,\ n = 1,\ldots,N \right\}.$$

The finite elements scheme we propose is the following.

Algorithm 1.

Step 1. *Set $j = 0$. Choose $\boldsymbol{m}_h^{(0)} = I_{\mathbb{V}_h}\boldsymbol{m}_0$.*

Step 2. *Find $\boldsymbol{v}_h^{(j+1)} \in \mathbb{W}_h^{(j)}$ satisfying*

$$\begin{aligned} &\alpha\left\langle \boldsymbol{v}_h^{(j+1)}, \boldsymbol{w}_h^{(j)} \right\rangle_\Omega + \left\langle \boldsymbol{m}_h^{(j)} \times \boldsymbol{v}_h^{(j+1)}, \boldsymbol{w}_h^{(j)} \right\rangle_\Omega \\ &\qquad = -\gamma\left\langle \nabla(\boldsymbol{m}_h^{(j)} + k\theta \boldsymbol{v}_h^{(j+1)}), \nabla \boldsymbol{w}_h^{(j)} \right\rangle_\Omega + \gamma\beta\left\langle J_h^{(j)}\cdot\nabla \boldsymbol{m}_h^{(j)}, \boldsymbol{w}_h^{(j)} \right\rangle_\Omega, \end{aligned} \tag{3}$$

for all $\boldsymbol{w}_h^{(j)} \in \mathbb{W}_h^{(j)}$.

Step 3. *Define*

$$\boldsymbol{m}_h^{(j+1)}(\boldsymbol{x}) := \sum_{n=1}^{N} \frac{\boldsymbol{m}_h^{(j)}(\boldsymbol{x}_n) + k\boldsymbol{v}_h^{(j+1)}(\boldsymbol{x}_n)}{|\boldsymbol{m}_h^{(j)}(\boldsymbol{x}_n) + k\boldsymbol{v}_h^{(j+1)}(\boldsymbol{x}_n)|}\phi_n(x).$$

Step 4. *Set $j = j+1$, and return to Step 2 if $j < M$. Stop if $j = M$.*

The parameter θ in (3) can be chosen arbitrarily in $[0,1]$. The method is explicit when $\theta = 0$ and semi-implicit when $\theta = 1$.

By the Lax–Milgram theorem, for each $j > 0$ there exists a unique solution $\boldsymbol{v}_h^{(j+1)} \in \mathbb{W}_h^{(j)}$ of equations (3) (see [1]). Since $|\boldsymbol{m}_h^{(j)}(\boldsymbol{x}_n)| = 1$ and $\boldsymbol{v}_h^{(j+1)}(\boldsymbol{x}_n) \cdot \boldsymbol{m}_h^{(j)}(\boldsymbol{x}_n) = 0$ for all $n = 1, \ldots, N$, there holds

$$|\boldsymbol{m}_h^{(j)}(\boldsymbol{x}_n) + k\boldsymbol{v}_h^{(j+1)}(\boldsymbol{x}_n)| \geq 1. \tag{4}$$

Therefore, the algorithm is well defined. There also holds $|\boldsymbol{m}_h^{(j+1)}(\boldsymbol{x}_n)| = 1$ for $n = 1, \ldots, N$.

4 Convergence to weak solutions

We start by recalling the following lemma proved in [6].

Lemma 1. *If there holds*

$$\int_\Omega \nabla \phi_i \cdot \nabla \phi_j \, dx \leq 0 \quad \textit{for all} \quad i, j \in \{1, 2, \ldots, M\} \textit{ and } i \neq j, \tag{5}$$

then for all $\boldsymbol{u} \in \mathbb{V}_h$ satisfying $|\boldsymbol{u}(\boldsymbol{x}_l)| \geq 1$, $l = 1, 2, \ldots, M$, there holds

$$\int_\Omega |\nabla I_h \left(\frac{\boldsymbol{u}}{|\boldsymbol{u}|} \right)|^2 \, dx \leq \int_\Omega |\nabla \boldsymbol{u}|^2 \, dx.$$

Condition (5) holds if all dihedral angles of the tetrahedra in $\mathscr{T}_h$ are less than or equal to $\pi/2$, see [6]. In the sequel we assume that (5) holds.

Lemma 2. *The solutions $(\boldsymbol{m}_h^{(j)}, \boldsymbol{v}_h^{(j+1)})$, $j = 0, 1, \ldots, M$, obtained from Algorithm 1 satisfy*

$$|\frac{\boldsymbol{m}_h^{(j+1)}(\boldsymbol{x}_n) - \boldsymbol{m}_h^{(j)}(\boldsymbol{x}_n)}{k}| \leq |\boldsymbol{v}_h^{(j+1)}(\boldsymbol{x}_n)|, \quad \forall n = 1, 2, \cdots, N, \quad j = 0, \ldots, M. \tag{6}$$

Proof. For the proof, see [23]. □

Now, we will show that our numerical solution converges to a weak solution of the problem (1). The next lemma provides a bound in the $\mathbb{L}^2$-norm for the discrete solutions.

Lemma 3. *The sequence $\left\{ \left(\boldsymbol{m}_h^{(j)}, \boldsymbol{v}_h^{(j+1)} \right) \right\}_{j=0,1,\ldots,M}$ produced by Algorithm 1 satisfies*

$$\mathscr{E}_h^{(j)} + C \sum_{i=0}^{j-1} k |\boldsymbol{v}_h^{(i+1)}|_\Omega^2 \leq \mathscr{E}_h^{(0)} \left(1 + \sum_{i=0}^{j-1} \frac{k\beta^2 |J_h^{(i)}|_\infty^2}{\alpha\gamma^{-1}} \exp\left(\sum_{s=0}^{i-1} \frac{k\beta^2 |J_h^{(s)}|_\infty^2}{\alpha\gamma^{-1}} \right) \right),$$

where

$$\mathscr{E}_h^{(j)} = |\nabla \boldsymbol{m}_h^{(j)}|_\Omega^2,$$

and

$$C = \begin{cases} \alpha\gamma^{-1} - (1 - 2\theta) C_1 k h^{-2}, & \theta \in [0, \frac{1}{2}), \\ \alpha\gamma^{-1}, & \theta \in [\frac{1}{2}, 1], \end{cases}$$

in which C_1 is a positive constant which is independent of j, k and h.

Proof. Choosing $\boldsymbol{w}_h^{(j)} = \boldsymbol{v}_h^{(j+1)}$ in (3), we obtain

$$\frac{\alpha}{\gamma}|\boldsymbol{v}_h^{(j+1)}|_\Omega^2 = -\left\langle \nabla(\boldsymbol{m}_h^{(j)} + k\theta \boldsymbol{v}_h^{(j+1)}), \nabla \boldsymbol{v}_h^{(j+1)} \right\rangle_\Omega + \beta \left\langle J_h^{(j)} \cdot \nabla \boldsymbol{m}_h^{(j)}, \boldsymbol{v}_h^{(j+1)} \right\rangle_\Omega,$$

which we write

$$\frac{\alpha}{\gamma}|\boldsymbol{v}_h^{(j+1)}|_\Omega^2 + k\theta|\nabla \boldsymbol{v}_h^{(j+1)}|_\Omega^2 = -\left\langle \nabla \boldsymbol{m}_h^{(j)}, \nabla \boldsymbol{v}_h^{(j+1)} \right\rangle_\Omega + \beta \left\langle J_h^{(j)} \cdot \nabla \boldsymbol{m}_h^{(j)}, \boldsymbol{v}_h^{(j+1)} \right\rangle_\Omega. \tag{7}$$

Since $\boldsymbol{m}_h^{(j)} + k\boldsymbol{v}_h^{(j+1)} \in \mathbb{V}_h$ and

$$\boldsymbol{m}_h^{(j+1)} = I_h\Big(\frac{\boldsymbol{m}_h^{(j)} + k\boldsymbol{v}_h^{(j+1)}}{|\boldsymbol{m}_h^{(j)} + k\boldsymbol{v}_h^{(j+1)}|}\Big),$$

it follows from (4) and Lemma 1 that

$$|\nabla \boldsymbol{m}_h^{(j+1)}|_\Omega^2 \leq |\nabla(\boldsymbol{m}_h^{(j)} + k\boldsymbol{v}_h^{(j+1)})|_\Omega^2.$$

Consequently, we have

$$|\nabla \boldsymbol{m}_h^{(j+1)}|_\Omega^2 \leq |\nabla \boldsymbol{m}_h^{(j)}|_\Omega^2 + k^2|\nabla \boldsymbol{v}_h^{(j+1)}|_\Omega^2 + 2k\left\langle \nabla \boldsymbol{m}_h^{(j)}, \nabla \boldsymbol{v}_h^{(j+1)} \right\rangle_\Omega. \tag{8}$$

Multiplying both sides of (7) by $2k$, we deduce

$$2k\gamma^{-1}\alpha|\boldsymbol{v}_h^{(j+1)}|_\Omega^2 + 2k^2\theta|\nabla \boldsymbol{v}_h^{(j+1)}|_\Omega^2 = -2k\left\langle \nabla m_h^{(j)}, \nabla \boldsymbol{v}_h^{(j+1)} \right\rangle_\Omega + 2k\beta\left\langle J_h^{(j)} \cdot \nabla \boldsymbol{m}_h^{(j)}, \boldsymbol{v}_h^{(j+1)} \right\rangle_\Omega, \tag{9}$$

Equality (8) is used to obtain from (9) the following inequality

$$|\nabla \boldsymbol{m}_h^{(j+1)}|_\Omega^2 \leq |\nabla \boldsymbol{m}_h^{(j)}|_\Omega^2 - k^2(2\theta-1)|\nabla \boldsymbol{v}_h^{(j+1)}|_\Omega^2 + 2k\beta\left\langle J_h^{(j)} \cdot \nabla \boldsymbol{m}_h^{(j)}, \boldsymbol{v}_h^{(j+1)} \right\rangle_\Omega - 2\alpha k\gamma^{-1}|\boldsymbol{v}_h^{(j+1)}|_\Omega^2.$$

Hence

$$\begin{aligned} &|\nabla \boldsymbol{m}_h^{(j+1)}|_\Omega^2 + k^2(2\theta-1)|\nabla \boldsymbol{v}_h^{(j+1)}|_\Omega^2 + 2\alpha k\gamma^{-1}|\boldsymbol{v}_h^{(j+1)}|_\Omega^2 \\ &\qquad \leq |\nabla \boldsymbol{m}_h^{(j)}|_\Omega^2 + 2k\beta\left\langle J_h^{(j)} \cdot \nabla \boldsymbol{m}_h^{(j)}, \boldsymbol{v}_h^{(j+1)} \right\rangle_\Omega. \end{aligned} \tag{10}$$

We have

$$2k\beta\left\langle J_h^{(j)} \cdot \nabla \boldsymbol{m}_h^{(j)}, \boldsymbol{v}_h^{(j+1)} \right\rangle_\Omega \leq 2k\beta|J_h^{(j)}|_\infty|\nabla \boldsymbol{m}_h^{(j)}|_\Omega|\boldsymbol{v}_h^{(j+1)}|_\Omega.$$

By Young inequality, we get

$$2k\beta|J_h^{(j)}|_\infty|\nabla \boldsymbol{m}_h^{(j)}|_\Omega|\boldsymbol{v}_h^{(j+1)}|_\Omega \leq \frac{k\beta^2|J_h^{(j)}|_\infty^2|\nabla \boldsymbol{m}_h^{(j)}|_\Omega^2}{\alpha\gamma^{-1}} + k\alpha\gamma^{-1}|\boldsymbol{v}_h^{(j+1)}|_\Omega^2.$$

Hence (10) gives

$$|\nabla \boldsymbol{m}_h^{(j+1)}|_\Omega^2 + k^2(2\theta-1)|\nabla \boldsymbol{v}_h^{(j+1)}|_\Omega^2 + \alpha k\gamma^{-1}|\boldsymbol{v}_h^{(j+1)}|_\Omega^2 \leq |\nabla \boldsymbol{m}_h^{(j)}|_\Omega^2 + \frac{k\beta^2|J_h^{(j)}|_\infty^2|\nabla \boldsymbol{m}_h^{(j)}|_\Omega^2}{\alpha\gamma^{-1}}.$$

Replacing j by i in the above inequality and summing over i from 0 to $j-1$ yields

$$|\nabla \boldsymbol{m}_h^{(j)}|_\Omega^2 + k^2(2\theta-1)\sum_{i=0}^{j-1}|\nabla \boldsymbol{v}_h^{(i+1)}|_\Omega^2 + \alpha\gamma^{-1}k\sum_{i=0}^{j-1}|\boldsymbol{v}_h^{(i+1)}|_\Omega^2$$
$$\leq |\nabla \boldsymbol{m}_h^{(0)}|_\Omega^2 + \frac{k\beta^2}{\alpha\gamma^{-1}}\sum_{i=0}^{j-1}|J_h^{(i)}|_\infty^2|\nabla \boldsymbol{m}_h^{(i)}|_\Omega^2. \tag{11}$$

When $\theta \in [\frac{1}{2}, 1]$, the term $k^2(2\theta-1)\sum_{i=0}^{j-1}|\nabla \boldsymbol{v}_h^{(i+1)}|_\Omega^2$ is nonnegative. So

$$|\nabla \boldsymbol{m}_h^{(j)}|_\Omega^2 + \alpha\gamma^{-1}\sum_{i=0}^{j-1}k|\boldsymbol{v}_h^{(i+1)}|_\Omega^2 \leq |\nabla \boldsymbol{m}_h^{(0)}|_\Omega^2 + \frac{k\beta^2}{\alpha\gamma^{-1}}\sum_{i=0}^{j-1}|J_h^{(i)}|_\infty^2|\nabla \boldsymbol{m}_h^{(i)}|_\Omega^2.$$

Therefore

$$|\nabla \boldsymbol{m}_h^{(i)}|_\Omega^2 \leq |\nabla \boldsymbol{m}_h^{(0)}|_\Omega^2 + \frac{k\beta^2}{\alpha\gamma^{-1}}\sum_{s=0}^{i-1}|J_h^{(i)}|_\infty^2|\nabla \boldsymbol{m}_h^{(s)}|_\Omega^2.$$

The discrete version of Gronwall's lemma allows to get

$$|\nabla \boldsymbol{m}_h^{(i)}|_\Omega^2 \leq |\nabla \boldsymbol{m}_h^{(0)}|_\Omega^2 \exp\Big(\sum_{s=0}^{i-1}\frac{k\beta^2|J_h^{(s)}|_\infty^2}{\alpha\gamma^{-1}}\Big).$$

Thus

$$|\nabla \boldsymbol{m}_h^{(j)}|_\Omega^2 + \alpha\gamma^{-1}\sum_{i=0}^{j-1}k|\boldsymbol{v}_h^{(i+1)}|_\Omega^2 \quad \leq |\nabla \boldsymbol{m}_h^{(0)}|_\Omega^2 + \frac{k\beta^2}{\alpha\gamma^{-1}}\sum_{i=0}^{j-1}|J_h^{(i)}|_\infty^2|\nabla \boldsymbol{m}_h^{(0)}|_\Omega^2 \exp\Big(\sum_{s=0}^{i-1}\frac{k\beta^2|J_h^{(s)}|_\infty^2}{\alpha\gamma^{-1}}\Big).$$

Then, we have

$$|\nabla \boldsymbol{m}_h^{(j)}|_\Omega^2 + C\sum_{i=0}^{j-1}k|\boldsymbol{v}_h^{(i+1)}|_\Omega^2 \leq |\nabla \boldsymbol{m}_h^{(0)}|_\Omega^2\Big(1+\sum_{i=0}^{j-1}\frac{k\beta^2|J_h^{(i)}|_\infty^2}{\alpha\gamma^{-1}}\exp\Big(\sum_{s=0}^{i-1}\frac{k\beta^2|J_h^{(s)}|_\infty^2}{\alpha\gamma^{-1}}\Big)\Big).$$

When $\theta \in [0, \frac{1}{2})$, we use the following inverse estimate (see for example [16]). On regular sequences of triangulations, there exists $C>0$ such that for all $\boldsymbol{v} \in \mathbb{V}_h$,

$$|\nabla \boldsymbol{v}_h^{(i)}|_\Omega^2 \leq Ch^{-2}|\boldsymbol{v}_h^{(i)}|_\Omega^2.$$

Applying the last inequality, we obtain

$$C_1K^2h^{-2}(2\theta-1)\sum_{i=0}^{j-1}k|\boldsymbol{v}_h^{(i+1)}|_\Omega^2 \leq k^2(2\theta-1)\sum_{i=0}^{j-1}|\nabla \boldsymbol{v}_h^{(i+1)}|_\Omega^2,$$

where C_1 is a positive constant which is independent of j, k and h. Hence from inequality (11), we obtain

$$|\nabla \boldsymbol{m}_h^{(j)}|_\Omega^2 + \big(\alpha\gamma^{-1} - C_1k^2h^{-2}(1-2\theta)\big)\sum_{i=0}^{j-1}k|\boldsymbol{v}_h^{(i+1)}|_\Omega^2 \leq |\nabla \boldsymbol{m}_h^{(0)}|_\Omega^2 + \frac{k\beta^2}{\alpha\gamma^{-1}}\sum_{i=0}^{j-1}|J_h^{(i)}|_\infty^2|\nabla \boldsymbol{m}_h^{(i)}|_\Omega^2.$$

The additional condition $k = o(h^2)$ assures us that $C = \alpha\gamma^{-1} - C_1K^2h^{-2}(1-2\theta)$ is positive when h and k are sufficiently small. Hence

$$|\nabla \boldsymbol{m}_h^{(j)}|_\Omega^2 + C\sum_{i=0}^{j-1} k|\boldsymbol{v}_h^{(i+1)}|_\Omega^2 \le |\nabla \boldsymbol{m}_h^{(0)}|_\Omega^2 + \frac{k\beta^2}{\alpha\gamma^{-1}}\sum_{i=0}^{j-1}|J_h^{(i)}|_\infty^2|\nabla \boldsymbol{m}_h^{(i)}|_\Omega^2.$$

Again, by the discrete version of Gronwall's lemma, we get

$$|\nabla \boldsymbol{m}_h^{(j)}|_\Omega^2 + C\sum_{i=0}^{j-1} k|\boldsymbol{v}_h^{(i+1)}|_\Omega^2 \le |\nabla \boldsymbol{m}_h^{(0)}|_\Omega^2\Big(1+\sum_{i=0}^{j-1}\frac{k\beta^2|J_h^{(i)}|_\infty^2}{\alpha\gamma^{-1}}\exp(\sum_{s=0}^{i-1}\frac{k\beta^2|J_h^{(s)}|_\infty^2}{\alpha\gamma^{-1}})\Big).$$

This completes the proof of the lemma. □

Remark 1. *The constant C in the above lemma is positive when $\theta \in [1/2,1]$. When $\theta \in [0,1/2)$ and the additional condition $\frac{k}{h^2}$ tends to zero as h and k go to 0 assures us that C is positive. This condition will be required later in the following lemma and theorem.*

Remark 2. *Note that in the approximation of the spin transfer torque (β-term) in (3) one may consider $\nabla(\boldsymbol{m}_h^{(j)} + k\theta\boldsymbol{v}_h^{(j+1)})$ instead of $\nabla\boldsymbol{m}_h^{(j)}$ but this choice seems to present some difficulty to get bound for approximate solutions.*

The discrete solutions $\boldsymbol{m}_h^{(j)}$ and $\boldsymbol{v}_h^{(j+1)}$ constructed via Algorithm 1 are interpolated in time in the following definition.

Definition 2. *For each $t \in [0,T]$, let $j \in \{0,\dots,M\}$ be such that $t \in [t_j, t_{j+1})$. We define for $t \in [0,T]$ and $x \in \Omega$*

$$\begin{aligned}
\boldsymbol{m}_{h,k}(t,x) &:= \frac{t-t_j}{k}\boldsymbol{m}_h^{(j+1)}(x) + \frac{t_{j+1}-t}{k}\boldsymbol{m}_h^{(j)}(x),\\
\boldsymbol{m}_{h,k}^-(t,x) &:= \boldsymbol{m}_h^{(j)}(x),\\
\boldsymbol{v}_{h,k}(t,x) &:= \boldsymbol{v}_h^{(j+1)}(x).
\end{aligned}$$

The following lemma shows that $\{\boldsymbol{m}_{h,k}\}$, $\{\boldsymbol{m}_{h,k}^-\}$ and $\{\boldsymbol{v}_{h,k}\}$ converge (up to the extraction of subsequences) as h and k tend to 0.

Lemma 4. *Assume that h and k go to 0 with a further condition $k = o(h^2)$ when $\theta \in [0,1/2)$ and no condition otherwise. There exists $\boldsymbol{m} \in \mathbb{H}^1(Q)$ such that*

$$\begin{cases}
\boldsymbol{m}_{h,k} \to \boldsymbol{m} \text{ strongly in } \mathbb{L}^2(Q),\\
\partial_t\boldsymbol{m}_{h,k} \rightharpoonup \partial_t\boldsymbol{m} \text{ weakly in } \mathbb{L}^2(Q),\\
\boldsymbol{v}_{h,k} \rightharpoonup \partial_t\boldsymbol{m} \text{ weakly in } \mathbb{L}^2(Q),\\
\boldsymbol{m}_{h,k}^- \to \boldsymbol{m} \text{ strongly in } \mathbb{L}^2(Q),\\
|\boldsymbol{m}| = 1 \text{ a.e. in } Q.
\end{cases}$$

Proof. From Lemma 2, we have

$$|\frac{\boldsymbol{m}_h^{(j+1)}(\boldsymbol{x}_n)-\boldsymbol{m}_h^{(j)}(\boldsymbol{x}_n)}{k}| \leq |\boldsymbol{v}_h^{(j+1)}(\boldsymbol{x}_n)| \quad \forall n=1,2,\ldots,N, \quad j=0,\ldots,M,$$

and since there exists $c>0$ such that for all $1 \leq p < +\infty$ and all $\phi_h \in \mathbb{V}_h$ holds

$$\frac{1}{c}\|\phi_h\|_{L^p(\Omega)}^p \leq h^d \sum_i \left|\phi_h\left(x_i^h\right)\right|^p \leq c\|\phi_h\|_{L^p(\Omega)}^p,$$

we obtain that

$$\left\|\frac{\boldsymbol{m}_h^{(j+1)}(\boldsymbol{x})-\boldsymbol{m}_h^{(j)}(\boldsymbol{x})}{k}\right\|_{L^2} \leq c^2\left\|v^{j+1}(\boldsymbol{x})\right\|_{L^2}.$$

Hence, from the bound

$$\mathscr{E}_h^{(j)} + C\sum_{i=0}^{j-1} k|\boldsymbol{v}_h^{(i+1)}|_\Omega^2 \leq \mathscr{E}_h^{(0)}\left(1+\sum_{i=0}^{j-1}\frac{k\beta^2|J_h^{(i)}|_\infty^2}{\alpha\gamma^{-1}}\exp(\sum_{s=0}^{i-1}\frac{k\beta^2|J_h^{(s)}|_\infty^2}{\alpha\gamma^{-1}})\right),$$

$m_{h,k}$ is uniformly bounded in $H^1(Q)$, and $v_{h,k}$ is bounded in $L^2(Q)$. Extracting possibly subsequences, there exist $m \in H^1(Q)$ and $v \in L^2(Q)$ such that

$$\begin{aligned} &m_{h,k} \to_{(h,k)\to 0} m \text{ weakly in } H^1(Q), \\ &m_{h,k} \to_{(h,k)\to 0} m \text{ strongly in } L^2(Q), \\ &v_{h,k} \to_{(h,k)\to 0} v \text{ weakly in } L^2(Q). \end{aligned}$$

Now, since for all $j=0,\cdots,J$ and all $t \in [jk,(j+1)k)$

$$\left|m_{h,k}(x,t)-m_{h,k}^-(x,t)\right| = \left|(t-jk)\left(\frac{m^{j+1}(x)-m^j(x)}{k}\right)\right| \leq k\left|\partial_t m_{h,k}(x,t)\right|,$$

we get

$$\left\|m_{h,k}-m_{h,k}^-\right\|_{L^2(Q)} \leq k\|\partial_t m_{h,k}\|_{L^2(Q)} \to_{(h,k)\to 0} 0.$$

Therefore

$$m_{h,k}^- \to_{(h,k)\to 0} m \text{ strongly in } L^2(Q).$$

Moreover, on any triangle (tetrahedron in 3D) K of $\mathscr{T}_h$, and any $u \in M_h$ one has, x_i^h being any vertex of K

$$||u(x)|-|u\left(x_i^h\right)||^2 \leq Ch^2|\nabla u|^2,$$

(recall that ∇u is constant on K), from which one deduces (since $\left|m_{h,k}^-\left(x_i^h\right)\right|=1$)

$$\int_{Q_T}|1-|m_{h,k}^-||^2 \leq Ch^2\|\nabla m_{h,k}^-\|_{L^2(Q)}^2,$$

which shows that

$$|m(x,t)|=1 \text{ a.e. } (x,t)\in Q.$$

Hence, the proof is completed. □

We are now ready to state the result of the convergence to weak solutions. Most of the arguments follow the same lines as in [1] and [23] to get:

Theorem 2. *Assume that h and k go to 0 with the following conditions*

$$\begin{cases} k = o(h^2), & \text{when } 0 \leq \theta < 1/2, \\ k = o(h), & \text{when } \theta = 1/2, \\ \text{no condition}, & \text{when } 1/2 < \theta \leq 1. \end{cases}$$

Then the limit $\boldsymbol{m}$ *given by Lemma 4 is a weak solution of the LLG Equation* (1).

5 Numerical experiments

For numerical experiments, we choose one dimensional geometry but the analysis can be performed for two or three dimensions. The one-dimensional spatial domain $\Omega = (0,1)$ is uniformly discretized with $x_i = ih$ and the mesh size $h = 1/10$. We set the values for the other parameters in (1) as $\alpha = 1$, $\gamma = 0.2$ and $\beta = 1$. We choose the time step $k = 10^{-3}$ and the parameter θ in Algorithm 1 to be 0.7. For the basis functions of the space $\mathbb{W}_h^{(j)}$, we make use of the construction proposed by Le-Tran [24]. At each iteration we need to solve a linear system of size $2(N+1) \times 2(N+1)$, where N is the number of nodes. As initial condition, we choose $\boldsymbol{m}_0(x) = (\cos \pi x, \sin \pi x, 0)$. The current J is assumed to flow with constant value to choose arbitrarily. The code is written in MATLAB®.

In a first set of experiments, Figure 1 shows the evolution of magnetization component averages. Switching is accompanied by oscillations which are the result of the magnetization precession around the effective field in the switching process. The amplitude of these oscillations tends to zero with an increasing number of averages. Note that for $J = 0$ (no injected current), magnetization field tends to align parallel to the nanowire axis (X-axis) while for the case with injected current magnetization tends to be in the XY plane between the X and Y axes. The simulations predict that large injected current favors alignement of magnetization with respect to Y axis.

In a second set of experiments to observe the boundedness of discrete energies, we solved the problem with a fixed value of h and smaller values of k. In Figure 2, we plotted $t \mapsto |\nabla \boldsymbol{m}_{h,k}(t)|_\Omega$ and the trajectory of the magnetization of a single domain particle on a large time scale ($T = 0.09$). Theoretically, the energy decay as time goes by. This is confirmed numerically indicating the energy relaxation. The time evolution of the energy is showed in Fig. 2 which seems to suggest that this energy approaches 0 for large time.

Figure 2 also shows the effect of the injected current in reaching equilibrium for magnetization field. We expect that increasing the current density shortens the switching time. We also remark that the magnetization approaches the final state faster in the presence of a spin transfer torque.

To demonstrate the dependence of the numerical approximations on the Gilbert damping, we tested the sensitivity of the solutions with respect to damping parameter. Figure 3 depicts for $J = 0.7$ the temporal evolution of the energy for $\alpha = 0.1$, $\alpha = 0.4$ and $\alpha = 0.8$. Figure 3 shows that as the damping increases the time needed by magnetization to reach equilibrium decreases.

To study the performance of the numerical scheme, we use the equivalent form equation of (1)

$$\partial_t \boldsymbol{m} = -\zeta \boldsymbol{m} \times (\triangle m + \beta (J \cdot \nabla) \boldsymbol{m}) - \mu \boldsymbol{m} \times (\boldsymbol{m} \times (\triangle m + \beta (J \cdot \nabla) \boldsymbol{m}), \tag{12}$$

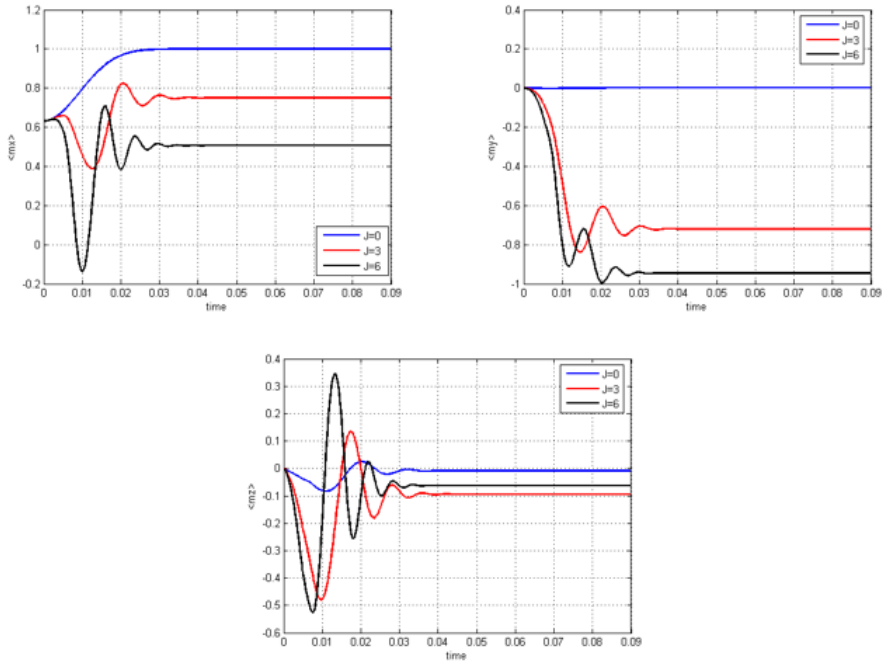

Figure 1: Averages of magnetization components $\langle m_x \rangle, \langle m_y \rangle$ and $\langle m_z \rangle$ for different values of J.

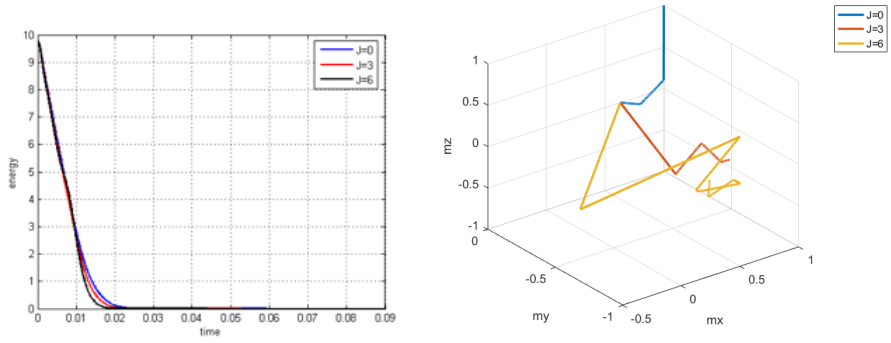

Figure 2: Temporal evolution of the energy in left and the trajectory of the magnetization of a single domain particle in right for $J = 0$, $J = 3$ and $J = 6$.

with $\zeta = \frac{\gamma}{1-\alpha^2}$ and $\mu = \frac{\alpha\gamma}{1-\alpha^2}$ see [36]. For $\zeta = 1$ and $\beta = 0$, the exact solution of (12) in one-dimensional space [15] is given by

$$m(t,x) = (m_1(t,x), m_2(t,x), m_3(t,x)),$$

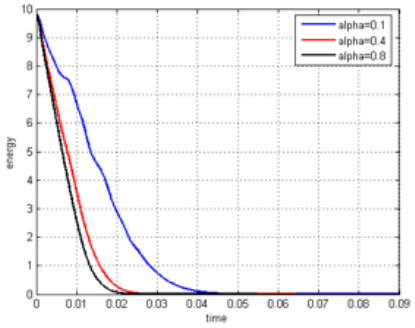

Figure 3: Temporal evolution of the energy for $\alpha = 0.1$, $\alpha = 0.4$ and $\alpha = 0.8$.

Table 1: Explicit method $(\theta = 0)$: L^∞ and L^2 error and convergence rates with spatial step h, time step $k = 8 \cdot 10^{-7} h^2$ and time 0.01.

$\frac{1}{h}$	$\left\|\mathbf{m}-\mathbf{m}^h\right\|_{L^\infty}$	$\left\|\mathbf{m}-\mathbf{m}^h\right\|_{L^2}$
32	8.50e^{-05}	7.40e^{-04}
64	2.06e^{-05}	1.75e^{-04}
128	5.65e^{-06}	4.90e^{-05}
256	1.73e^{-06}	1.19e^{-05}

where

$$m_1(t,x) = \frac{\sin\varphi\ \cos(kx-\phi(x,t,\varphi,k,\mu))}{d(t,\varphi,k,\mu)},$$
$$m_2(t,x) = \frac{\sin\varphi\ \sin(kx-\phi(x,t,\varphi,k,\mu)}{d(t,\varphi,k,\mu)},$$
$$m_3(t,x) = \frac{\exp(k^2\mu t)\cos\varphi}{d(t,\varphi,k,\mu)},$$

with

$$d(t,\alpha,k,\mu) = \sqrt{\sin^2\varphi + \exp(2k^2\mu t)\cos^2\varphi},$$

and

$$\phi(x,t,\varphi,k,\mu) = \frac{1}{\mu}\log\left(\frac{d(t,\varphi,k,\mu)+\exp(k^2\mu t)\cos\varphi}{1+\cos\varphi}\right),$$

where $\varphi = \frac{\pi}{24}$ and $k = 2\pi$. For the convergence study, we used an explicit method $(\theta = 0)$ and an implicit method $(\theta = 0.5)$. The L^∞ and L^2 errors were measured relative to an exact solution of the Landau-Lifshitz equation. The numerical results are summarized in the Tables 1 and 2. Figure 4 shows the convergence rate of the method, which is first order in the time step k and second order in the mesh size h.

Table 2: Implicit method $(\theta = \frac{1}{2})$: L^∞ and L^2 error and convergence rates with spatial step h, time step $k = 8 \cdot 10^{-7} h^2$ and time 0.01.

$\frac{1}{h}$	$\left\|\mathbf{m}-\mathbf{m}^h\right\|_{L^\infty}$	$\left\|\mathbf{m}-\mathbf{m}^h\right\|_{L^2}$
32	7.96e^{-05}	7.89e^{-04}
64	3.87e^{-05}	1.58e^{-04}
128	5.78e^{-06}	5.09e^{-05}
256	1.07e^{-06}	0.92e^{-05}

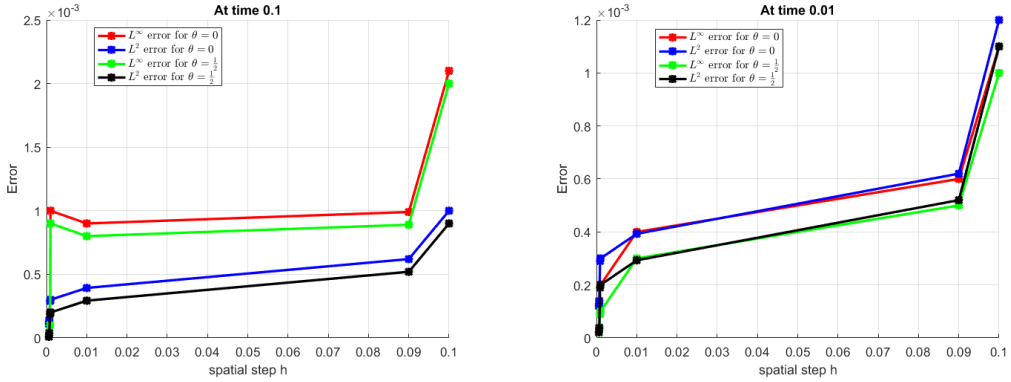

Figure 4: Convergence plot, Left : At time 0.1, Right : At time 0.01.

6 Concluding remarks

The main goal is to understand the behaviour of magnetic moments caused by spin polarized current. We have considered a mathematical model consisting of a generalized LLG equation incorporating adiabatic spin torque term expressed as a transport term in the effective field. A finite element approximation is proposed and the convergence of the approximate solutions to a weak solution is proved. Numerical experiments are carried out to show the effect of the injected current in reaching equilibrium for magnetization field. We expect that the switching time depends on the applied current density which shortens the time switching. The code developed in this paper may be used especially to describe domain wall motion in nanowires since a one-dimensional approximation of the magnetostatic field is known, see for example [9]. In order to complete the study we intend to extend our implementation to higher dimensions by incorporating all the energetic contributions including the energy of anisotropy and demagnetization. One may then examine the importance of these energies respectively, by deliberately removing one or both of them in the magnetization switching process. Note that within the second-order gradient, it is found in [34] that the LLG equation should be modified by adding to effective field a term of the form $\beta \boldsymbol{m} \times \triangle \boldsymbol{m}$. This new field is vertical to the plane defined by the magnetization and the normal spin stiffness $\triangle \boldsymbol{m}$ [34]. In this case, the LLG equation becomes

$$\partial_t \boldsymbol{m} - \alpha \boldsymbol{m} \times \partial_t \boldsymbol{m} = -\gamma \boldsymbol{m} \times (\mathscr{H}_e + \beta \boldsymbol{m} \times \triangle \boldsymbol{m}).$$

Interestingly, the vertical spin stiffness can not be written in terms of the free energy, and therefore, it can not be derived from the functional derivative of the free energy with respect to the local magnetization.

This new term can significantly change the domain-wall structure in ferromagnetic materials. It would be interesting to consider this problem both from the theoretical and numerical points of view.

In the end, we would like to point out that there is no theoretical difficulties to extend this study to the non-adiabatic torque considered in [27] and the competition between Gilbert damping and spin transfer torques in magnetization dynamics should be characterized for a good understanding of the switching process.

References

[1] F. Alouges, *A new finite element scheme for Landau-Lifchitz equations,* Discrete Contin. Dyn. Syst. Ser. S. **1** (2008) 187–196.

[2] F. Alouges, P. Jaisson, *Convergence of a finite element discretization for the Landau-Lifshitz equations in micromagnetism,* Math. Models Methods Appl Sci. **6** (2006) 299–316.

[3] F. Alouges, A. Soyeur, *On global weak solutions for Landau-Lifshitz equations: Existence and non uniqueness,* Nonlinear Anal. **18** (1992) 1071–1084.

[4] L. Banas, S. Bartels, A. Prohl, *A convergent implicit finite element discretization of the Maxwell–Landau–Lifshitz–Gilbert equation,* SIAM J. Numer. Anal. **46** (2008) 1399–1422.

[5] L. Banas, M. Page, D. Praetorius, *A convergent linear finite element scheme for the Maxwell–Landau–Lifshitz–Gilbert equation,* arXiv:1303.4009, 2012.

[6] S. Bartels, *Stability and convergence of finite-element approximation schemes for harmonic maps,* SIAM J. Numer. Anal. **43** (2005) 220–238.

[7] L. Berger, *Emission of spin waves by a magnetic multilayer traversed by a current,* Phys. Rev. B **54** (1996) 9353.

[8] G. Carbou, P. Fabrie, *Regular solutions for Landau-Lifschitz equation in a bounded domain,* Differ. Integral Equ. **14** (2001) 213–229.

[9] G. Carbou, S. Labbe, E. Trelat, *Control of travelling walls in a ferromagnetic nanowire,* Discrete Contin. Dyn. Syst. Ser. S **1** (2008) 51–59.

[10] M. Hamid, M. Usman, R.Ul. Haq, Z. Tian, *A spectral approach to analyze the nonlinear oscillatory fractional-order differential equations,* Chaos Solitons and Fractals **146** (2021) 110921.

[11] M. Hamid, M. Usman, R.U. Haq, Z. Tian, W. Wang, *Linearized stable spectral method to analyze two-dimensional nonlinear evolutionary and reaction-diffusion models,* Numer. Methods Partial Differ. Equations (2020) 1-19.

[12] M. Hamid, M. Usman, Z. Tian, W. Wang, *A stable computational approach to analyze semi-relativistic behavior of fractional evolutionary problems,* Numer. Methods Partial Differ. Equations (2008) 1–15.

[13] M. Hamid, M. Usman, Z. Tian, W. Wang, *Hybrid fully spectral linearized scheme for time-fractional evolutionary equations,* Math. Methods Appl. Sci. **44** (2021) 3890–3912.

[14] M. Hamid, M. Usman, T. Zubair, R.l. Haq, A. Shafee, *An efficient analysis for N-soliton, Lump and lump–kink solutions of time-fractional (2+ 1)-Kadomtsev–Petviashvili equation,* Physica A Stat. Mech. Appl. **528** (2019) 121320.

[15] D. Jeong, J. Kim, *An accurate and robust numerical method for micromagnetics simulations,* Curr. Appl. Phys. **14** (2014) 476–483.

[16] C. Johnson, *Numerical Solution of Partial Differential Equations by the Finite Element Method,* Cambridge University Press, Cambridge. 1987.

[17] A. Khodadadian, K. Hosseini, A. Manzour-ol-Ajdad, M. Hedayati, R. Kalantarinejad, C. Heitzinger, *Optimal design of nanowire field-effect troponin sensors,* Comput. Biol. Med. Comput. Biol. Med. **87** (2017) 46–56.

[18] A. Khodadadian, M. Parvizi, C. Heitzinger, *An adaptive multilevel Monte Carlo algorithm for the stochastic drift-diffusion-Poisson system,* Comput. Methods Appl. Mech. Engrg. **368** (2020) 113163.

[19] A. Khodadadian, L. Taghizadeh, C. Heitzinger, *Three-dimensional optimal multi-level Monte–Carlo approximation of the stochastic drift–diffusion–Poisson system in nanoscale devices,* J. Comput. Electron. **17** (2018) 76–89.

[20] H. Kohno, G. Tatara, J. Shibata, Y. Suzuki, *Microscopic Calculation of Spin Torques and Forces,* J. Magn. Magn. Mater. **310** (2006) 2020–2022.

[21] M. Kruzik, A. Prohl, *Recent developments in the modeling, analysis, and numerics of ferromagnetism,* SIAM Rev. **48** (2006) 439–483.

[22] S. Labbe, *Fast computation for large magnetostatic systems adapted for micromagnetism,* SIAM J. Sci. Comput. **26** (2005) 2160–2175.

[23] K.-N. Le, T. Tran, *A convergent finite element approximation for the quasi-static Maxwell-Landau-Lifshitz-Gilbert equations,* Comput. Math. Appl. **66** (2013) 1389–1402.

[24] K.N. Le, T. Tran, *A finite element approximation for the quasi-static Maxwell–Landau–Lifshitz–Gilbert equations,* ANZIAM J. **54** (2012) C681–C698.

[25] J. Liu, Z. Zhou, *Finite element approximation of time fractional optimal control problem with integral state constraint [J],* AIMS Mathematics **6** (2021) 979–997.

[26] L. Lu, X. Meng, Z. Mao, G.E. Karniadakis, *DeepXDE: a deep learning library for solving differential equations,* SIAM Rev. **63** (2021) 208–228.

[27] C. Melcher, M. Ptashnyk, *Landau-Lifshitz-Slonczewski equations: global weak and classical solutions,* SIAM J. Math. Anal. **45** (2013) 407–429,.

[28] S. Mirsian, A. Khodadadian, M. Hedayati, A. Manzour-ol-Ajdad, R. Kalantarinejad, C. Heitzinger, *A new method for selective functionalization of silicon nanowire sensors and Bayesian inversion for its parameters,* Biosens. Bioelectron. **142** (2019) 111527.

[29] M. Moumni, M. Tilioua, *A finite-difference scheme for a model of magnetization dynamics with inertial effects,* J. Eng. Math. **100** (2016) 95–106.

[30] B. Nkemzi, M. Jung, *Singular solutions of the Poisson equation at edges of three-dimensional domains and their treatment with a predictor–corrector finite element method,* Numer. Methods Partial. Differ. Equ. **37** (2021) 836–853.

[31] M. Parvizi, A. Khodadadian, M. R. Eslahchi, *Analysis of Ciarlet-Raviart mixed finite element methods for solving damped Boussinesq equation,* J. Comput. Appl. Math. **379** (2020) 112818.

[32] L. Qian, S. Dongyang. *Superconvergent analysis of a nonconforming mixed finite element method for time-dependent damped Navier–Stokes equations,* Comput. Appl. Math. **40** (2021) 1–17.

[33] M. Raissi, G.E. Karniadakis, *Hidden physics models: Machine learning of nonlinear partial differential equations,* J. Comput. Phys. **357** (2018) 125–141.

[34] K. Shen, G. Tatara, M.W. Wu, *Existence of vertical spin stiffness in Landau-Lifshitz-Gilbert equation in ferromagnetic semiconductors,* Phys. Rev. B. **83** (2011) 085203.

[35] J.C. Slonczewski, *Current-driven excitation of magnetic multilayer,* J. Magn. Magn. Mater. **159** (1996) L1–L7.

[36] M. Tilioua, *Comportement asymptotique de materiaux ferromagntiques minces avec energie de surface et/ou couplage dechange inter-couches,* PhD thesis, Palaiseau, Ecole polytechnique, 2003.

[37] M. Tilioua, *Current-induced magnetization dynamics. Global existence of weak solutions,* J. Math. Anal. Appl. **373** (2011) 635–642.

[38] A. Visintin, *On the Landau-Lifshitz equation for ferromagnetism,* Japan J. Appl. Math. **2** (1985) 69–84.

[39] E. Weinan, J. Han, A. Jentzen, *Deep learning-based numerical methods for high-dimensional parabolic partial differential equations and backward stochastic differential equations,* Commun. Math. Stat. **5** (2017) 349–380.